Figures and figure supplements

Claudin5 protects the peripheral endothelial barrier in an organ and vessel type-specific manner

Mark Richards *et al*

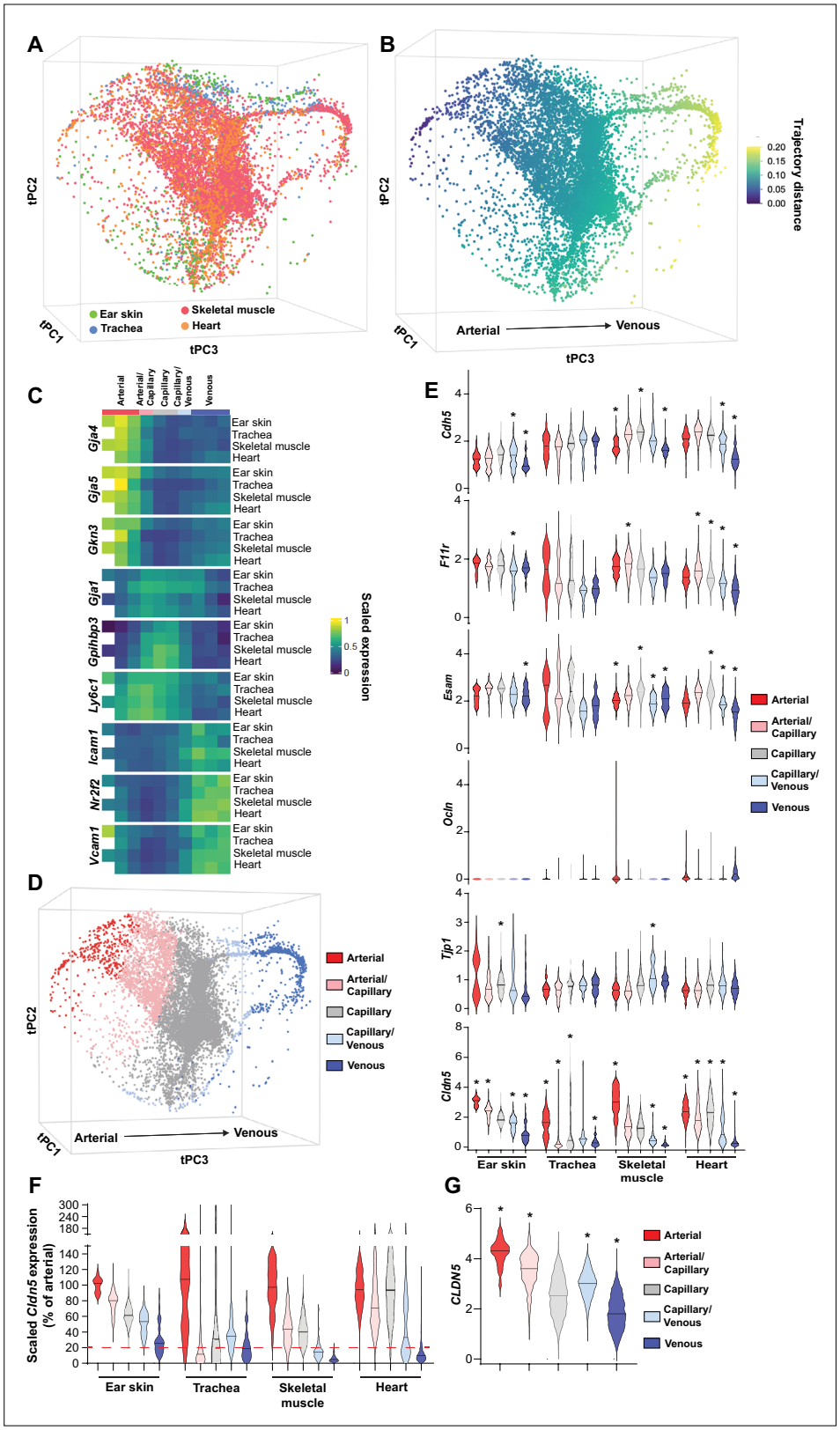

Figure 1. Patterning of the EC barrier at the single-cell level. (**A**) Principal component analysis of the distances within 400 trajectories calculated with integrated data of murine datasets of ear skin, trachea, skeletal muscle, and heart blood endothelial cells (BECs). Colours illustrate the distribution of BECs (CD31+/CD45-/Lyve1-) for each organ. (**B**) Principal component analysis of trajectory distances coloured by the distance along an isolated

Figure 1 continued on next page

Figure 1 continued

trajectory spanning from arterial to venous BEC. (**C**) Mean gene expression for each organ after equidistant binning of the isolated trajectory shown in B. Supervised vessel subset specifications (Top) based on the expression of previously established marker genes. (**D**) Principal component analysis of trajectory distances coloured by the vessel subsets defined in C. (**E**) Violin plots of gene expression for BEC junctional components. Gene expression was normalized to account for differences in sample library size and has been imputed to account for dropouts in the data as described in Methods. (**F**) *Cldn5* expression in murine BEC datasets scaled per organ according to the mean expression in the arterial BECs of each organ. Red dashed line represents a 5-fold reduction in expression compared to arterial BECs. (**G**) *CLDN5* expression in human dermal BECs. n=534 ear skin, 559 trachea, 3,498 skeletal muscle, 6,423 heart and 8,518 human BEC. * denotes statistical significance following differential gene expression analysis (***Figure 1—source data 1–5***).

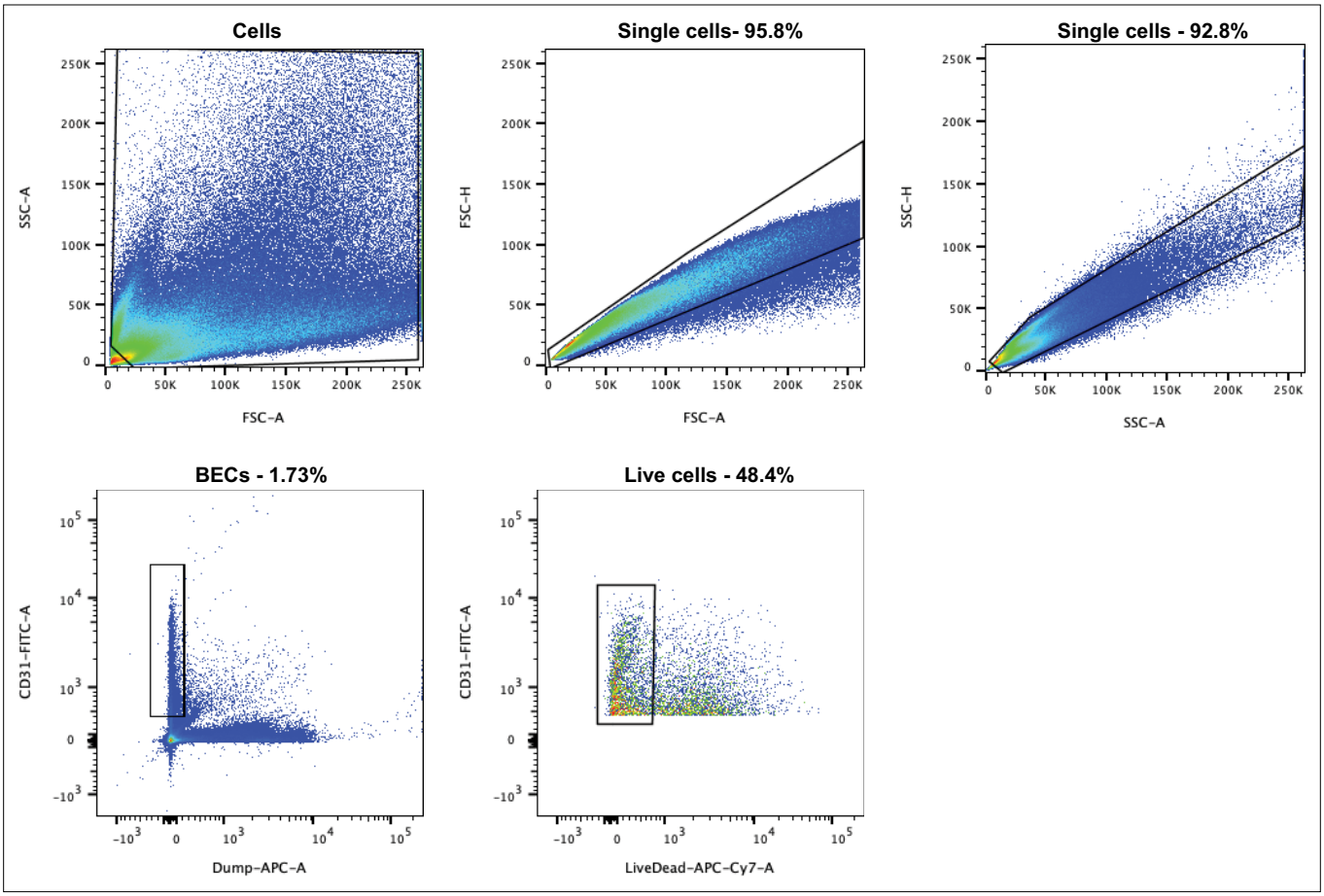

Figure 1—figure supplement 1. Gating strategy for the FACS isolation of single blood vessel BECs from the mouse ear skin.

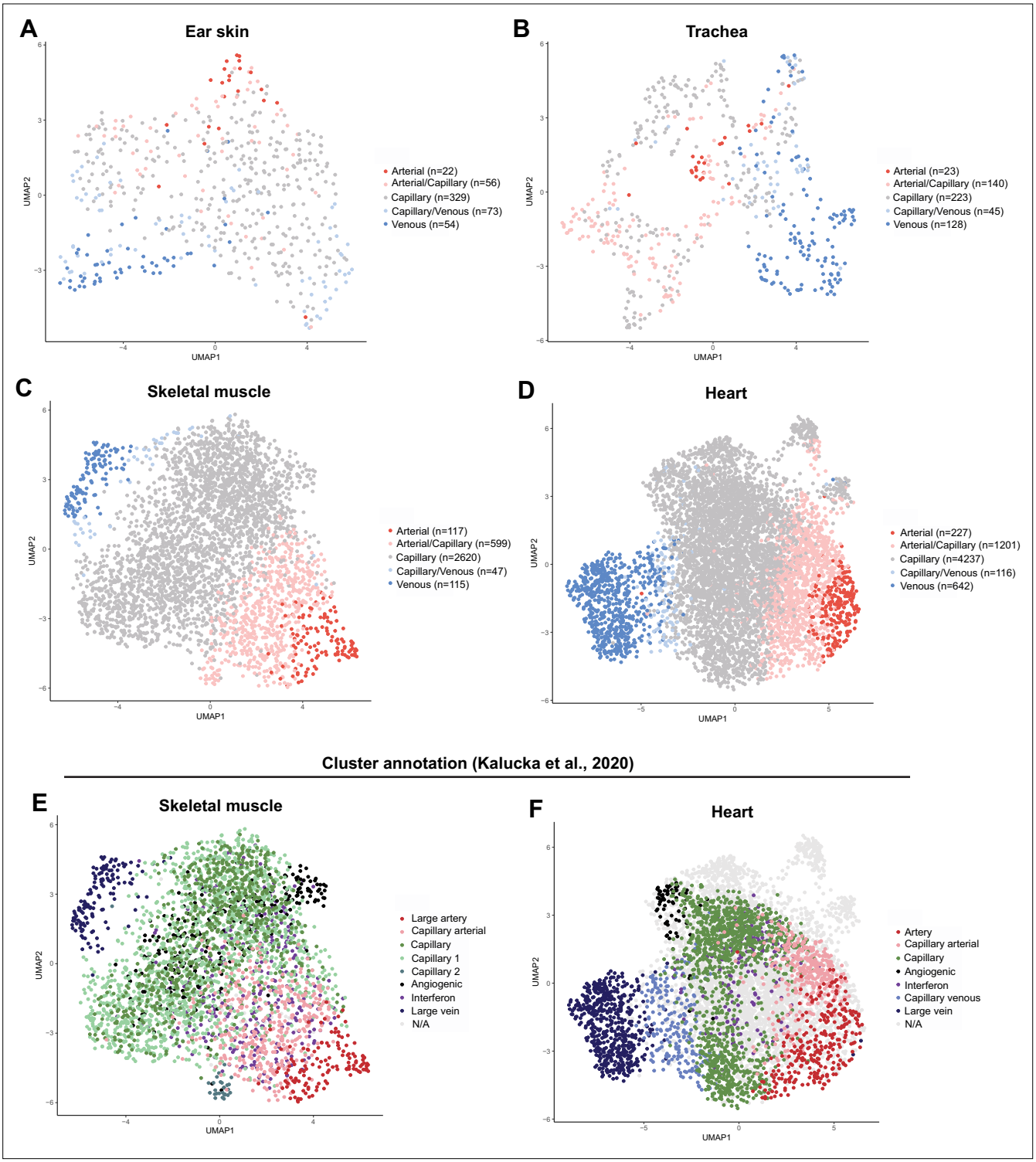

Figure 1—figure supplement 2. (**A**) Ear skin, (**B**) trachea, (**C**) skeletal muscle and (**D**) heart mouse BECs coloured by subset as defined by analysis of integrated data. The number of cells in each subtype are specified in each legend. (**E**) Skeletal muscle and (**F**) heart mouse BECs coloured by clusters identified in the original publication of the data (***Kalucka et al., 2020***).

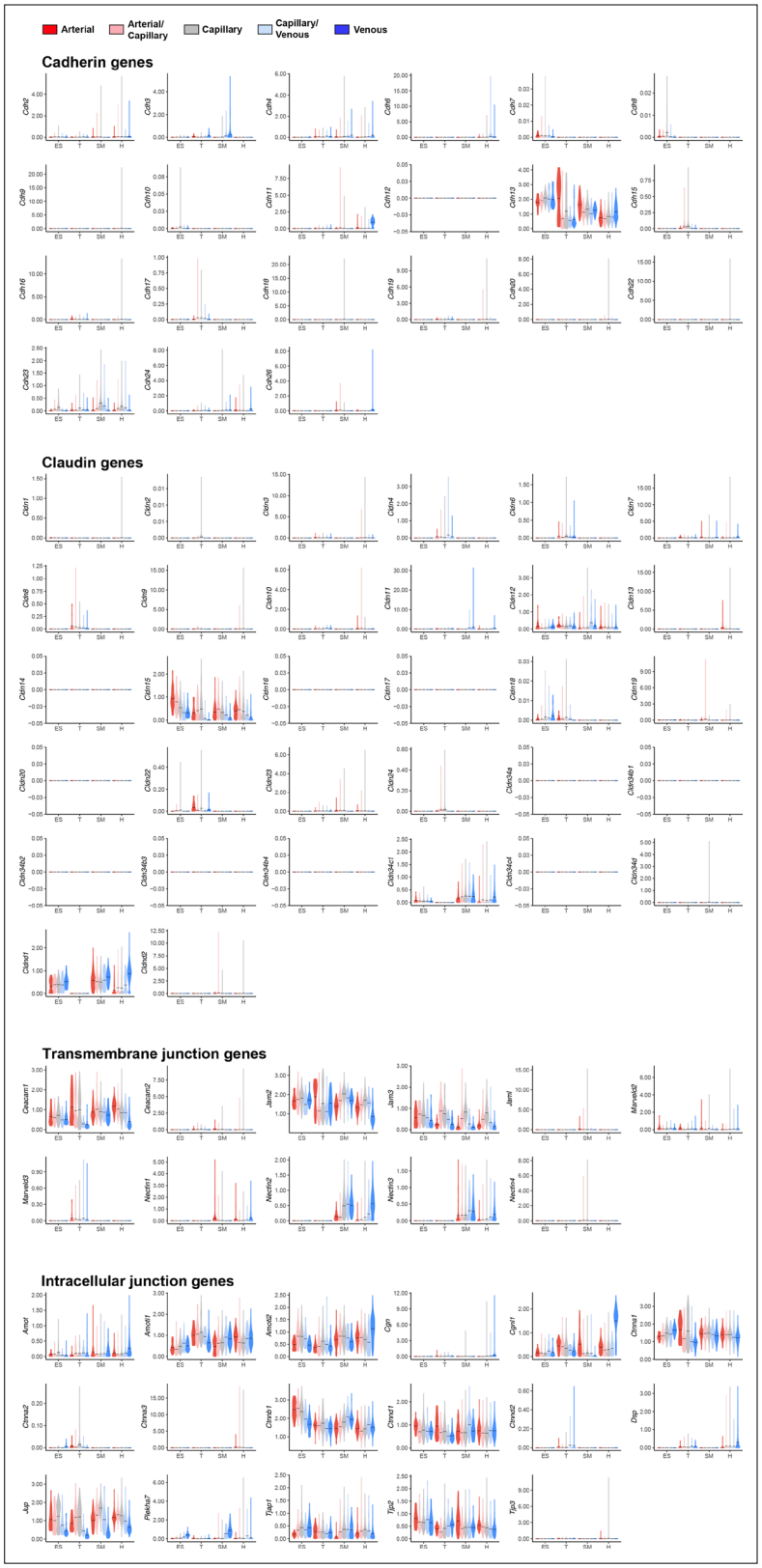

Figure 1—figure supplement 3. Violin plots of gene expression for mouse endothelial junctional components. Gene expression was normalized to account for differences in sample library size and imputed to account for dropouts in the data as described in Methods. ES, ear skin; T, trachea; SM, skeletal muscle; H, heart.

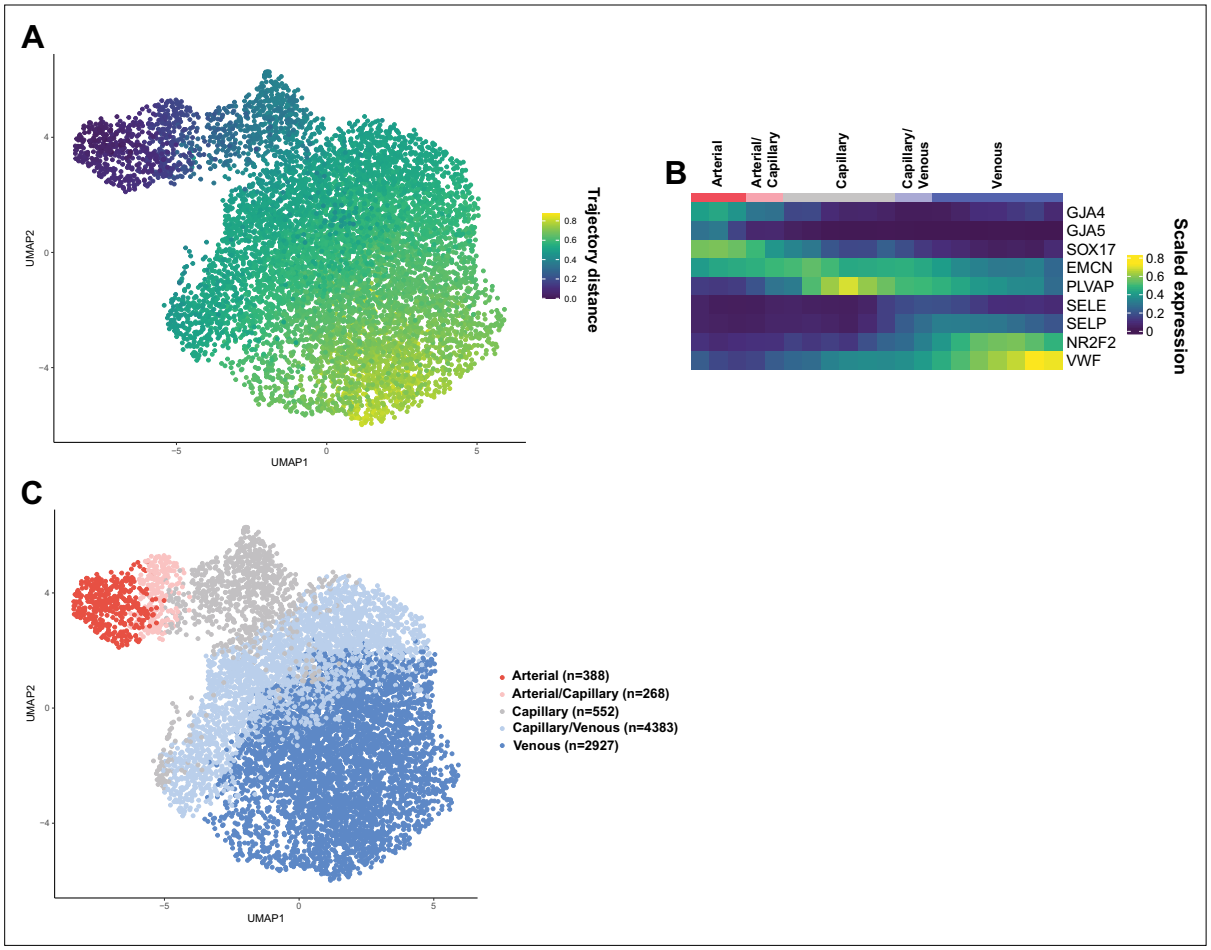

Figure 1—figure supplement 4. (**A**) Uniform manifold approximation and projection (UMAP) of human dermal BECs showing the distance of an isolated trajectory calculated with tSpace. (**B**) Equidistant binning of the trajectory shown in A. with supervised annotation of the bins as vessel subsets. (**C**) UMAP coloured by the vessel subsets specified in B.

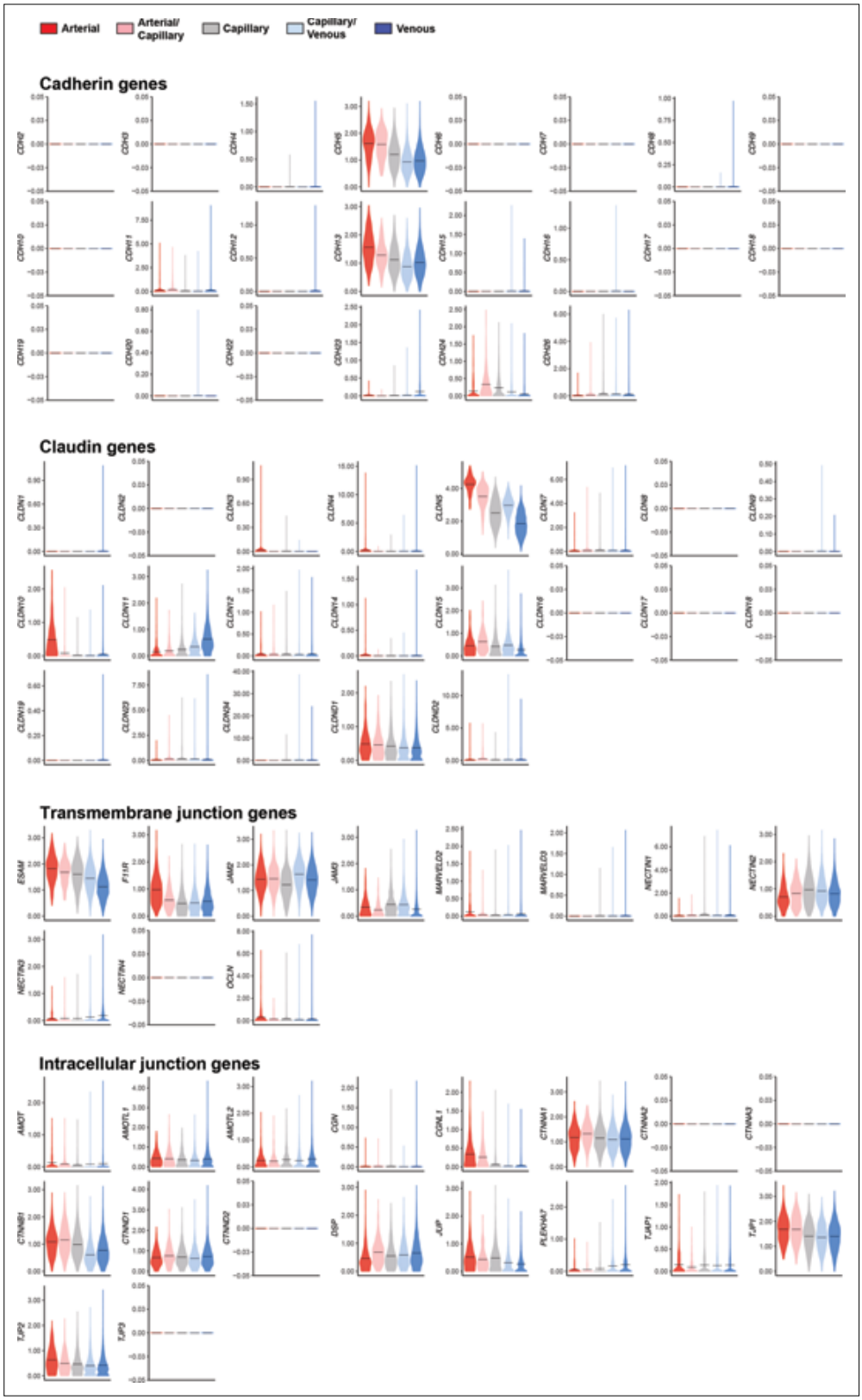

Figure 1—figure supplement 5. Violin plots of gene expression for human dermal endothelial junctional components. Gene expression was normalized to account for differences in library size and imputed to account for dropouts in the data as described in Methods.

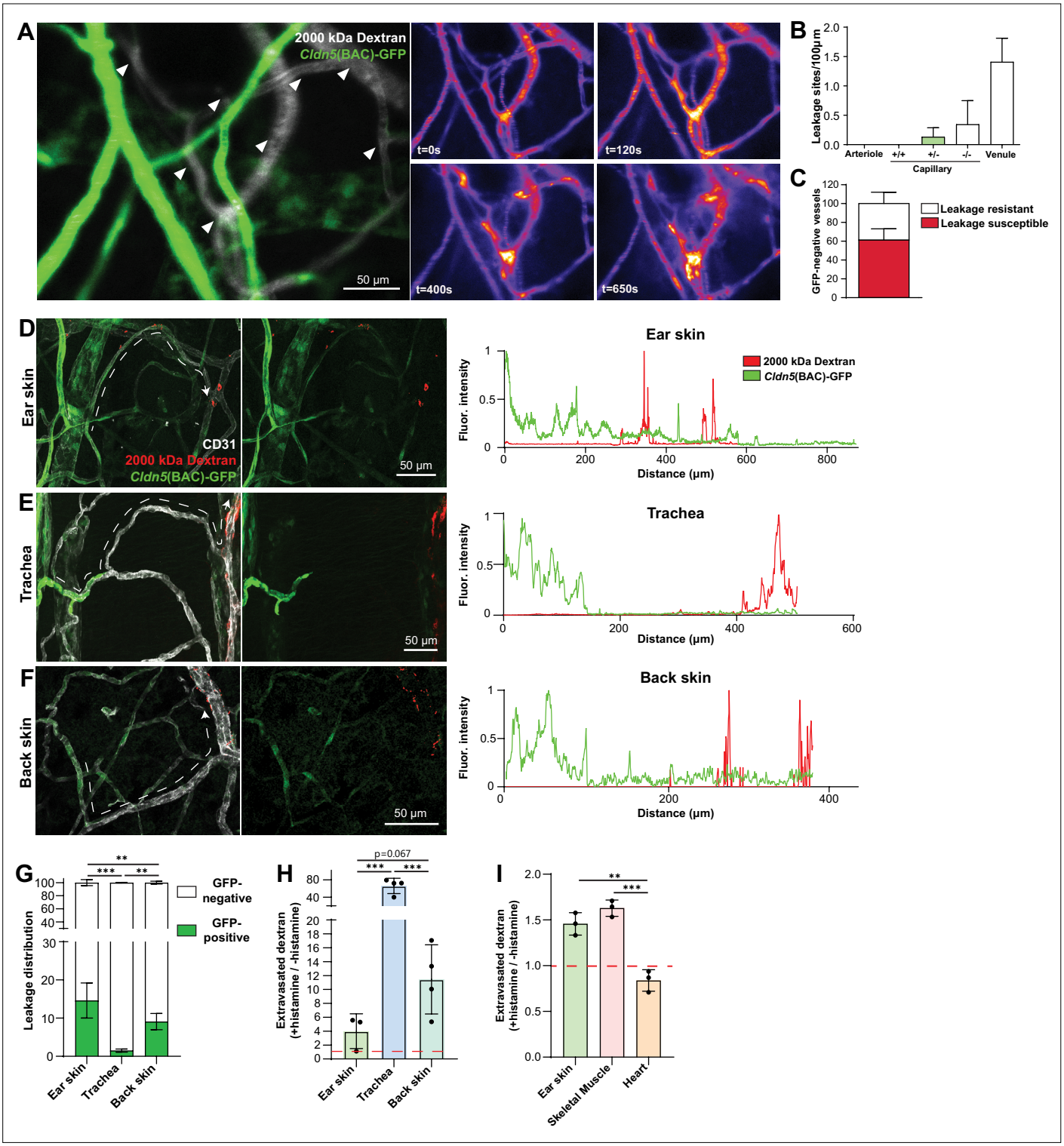

Figure 2. Organotypic integrity of the EC barrier. (**A**) Leakage patterning in *Cldn5*(BAC)-GFP mouse ear skin in response to intradermal histamine. Left, overlay of *Cldn5*(BAC)-GFP-positive and -negative vessels (visualised through circulating TRITC dextran). Arrowheads show sites of leakage. Right, stills of leakage in the vasculature shown on the left following intradermal histamine stimulation. (**B**) Leakage sites per vessel length in different vessel categories. +/+denotes capillary segments with full GFP expression,+/-denotes capillary segments with mixed GFP expression, -/- denotes capillary segments with no GFP expression. n=4, 2 or more acquisitions/mouse. (**C**) Proportion of *Cldn5*(BAC)-GFP-negative vessels susceptible or resistant to leakage. n=4, 2 or more acquisitions/mouse. (**D–F**) Leakage patterning in the ear skin (**D**), trachea (**E**) and back skin (**F**) in response to the systemic administration of histamine. Left, representative image. Dashed line shows progression of a blood vessel from arteriolar to venular. Right, representative

Figure 2 continued on next page

Figure 2 continued

fluorescent intensity line profile of *Cldn5*(BAC)-GFP and TRITC 2000 kDa dextran along the dashed line (Left). (**G**) Proportion of 2000 kDa FITC leakage area that occurs in vessels that are *Cldn5*(BAC)-GFP-positive (contain some positive cells) and *Cldn5*(BAC)-GFP-negative (contain no positive cells) in ear skin, back skin and trachea. n≥3 mice, 3 or more fields of view/mouse. (**H**) Fold change in 2000 kDa TRITC dextran extravasation from leakage permissive vessels in ear skin, back skin and trachea with and without systemic histamine stimulation. Dashed line represents unstimulated tissue. n=3 mice, 3 or more fields of view/mouse. (**I**) Fold change in tissue 2000 kDa FITC dextran following systemic histamine stimulation and formamide extraction of ear skin, skeletal muscle and heart. Dashed line represents unstimulated tissue. n=3 mice. Error bars; mean ± SD. Statistical significance: one-way ANOVA with Tukey's post-hoc test (multiple comparisons; **G–I**).

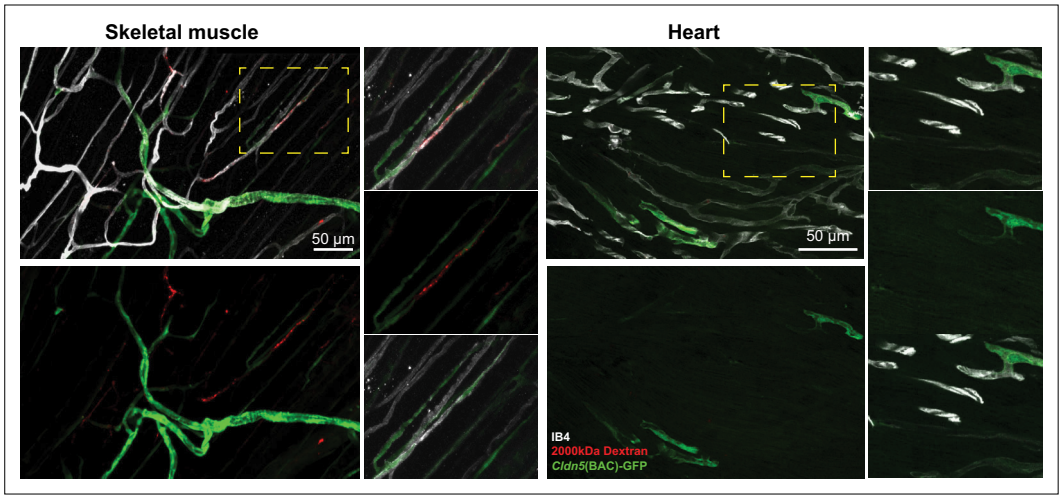

Figure 2—figure supplement 1. Leakage and *Cldn5*(BAC)-GFP expression patterning in skeletal muscle and heart in response to the systemic administration of histamine. Magnified images of dashed boxes are shown to the right of the main image.

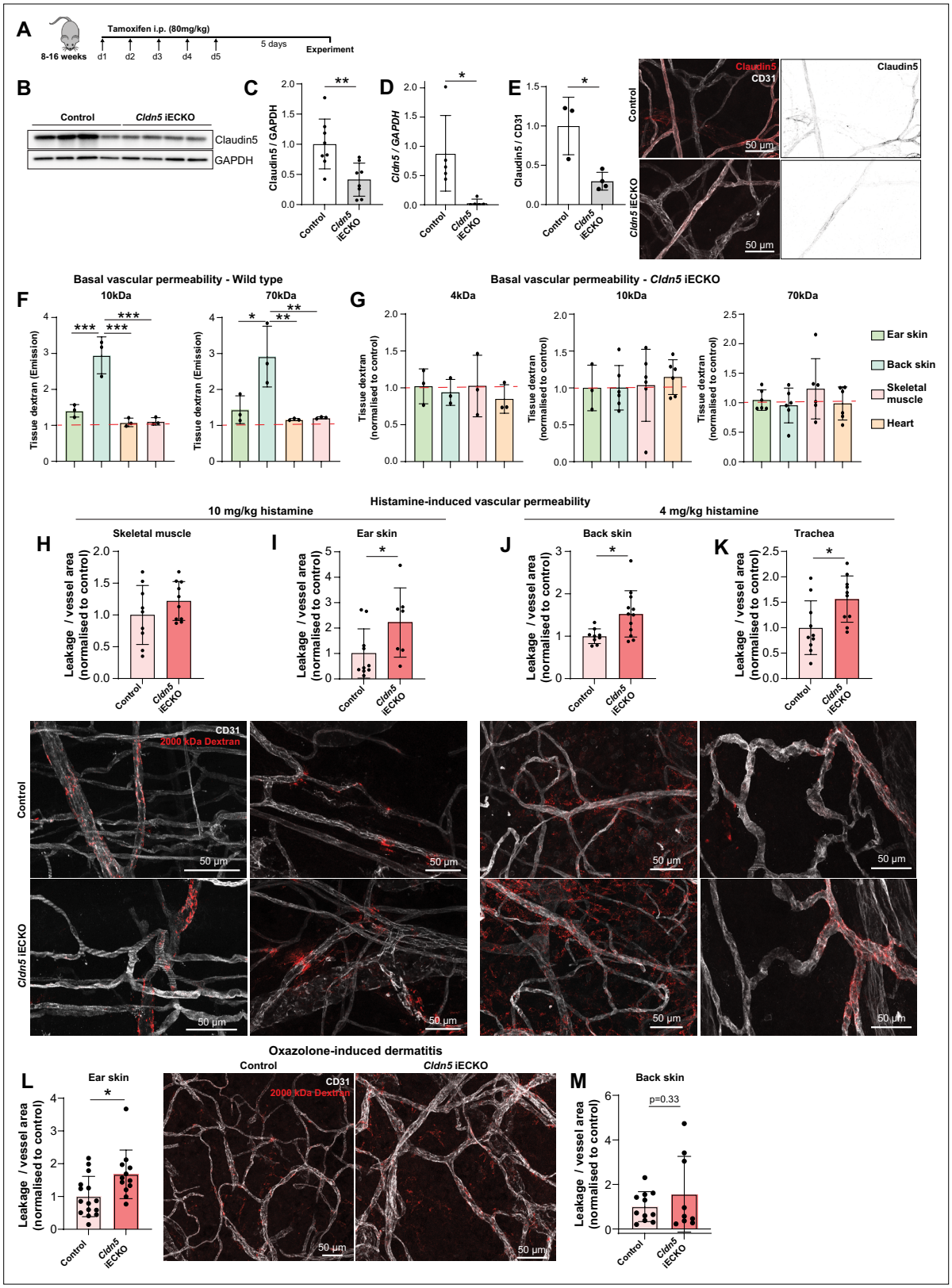

Figure 3. Claudin5 exhibits organotypic protection of the EC barrier. (**A**) Schematic illustration of systemic tamoxifen regime. (**B**) Representative western blot of Claudin5 protein expression in control and *Cldn5* iECKO mice. (**C**) Quantification of Claudin5 protein expression in lung lysates of control and *Cldn5* iECKO mice. n≥8 mice. (**D**) *Cldn5* gene expression by qPCR on lung lysates of control and *Cldn5* iECKO mice. n≥5 mice. (**E**) Claudin5 protein expression normalized to CD31 counter-staining in the ear skin of control and *Cldn5* iECKO mice following systemic tamoxifen. Right, representative

Figure 3 continued on next page

Figure 3 continued

images of Claudin5 immunostaining in control and *Cldn5* iECKO mice. n≥3 mice, 3 or more fields of view/mouse. (**F**) Blood vessel basal permeability to 10 kDa and 70 kDa dextran in ear skin, back skin, skeletal muscle and heart of wildtype C57Bl/6 mice. Dashed lines represent background from control uninjected mice. n=3 mice. (**G**) Blood vessel basal permeability to 4 kDa, 10 kDa and 70 kDa dextran in ear skin, back skin, skeletal muscle and heart of control and *Cldn5* iECKO mice. Dashed lines represent control Cre-negative mice. n≥3 mice. (**H–I**) Leakage of 2000 kDa dextran in response to systemic histamine stimulation (10 mg/kg) in skeletal muscle (**H**) and ear skin (**I**). Top, quantification of tracer leakage area / vessel area normalised to control (Cre-negative) mice. Bottom, representative images. n≥7 mice, 3 or more fields of view/mouse. (**J–K**) Leakage of 2000 kDa dextran in response to systemic histamine stimulation (4 mg/kg) in back skin (**J**) and trachea (**K**). Top, quantification of tracer leakage area / vessel area normalised to control (Cre-negative) mice. Bottom, representative images. n≥8 mice, 3 or more fields of view/mouse. (**L**) Quantification of 2000 kDa dextran leakage in the ear skin of control and *Cldn5* iECKO mice following Oxazolone-induced dermatitis. Right, representative images. n≥12 mice, 2 or more fields of view/mouse (**M**) Quantification of 2000 kDa dextran leakage in the back skin of control and *Cldn5* iECKO mice following Oxazolone-induced dermatitis. n≥9 mice, 2 or more fields of view/mouse Error bars; mean ± SD. Statistical significance: two-tailed paired Student's t test (**C-E**), H-M or one-way ANOVA with Tukey post-hoc test (multiple comparisons; **F–G**).

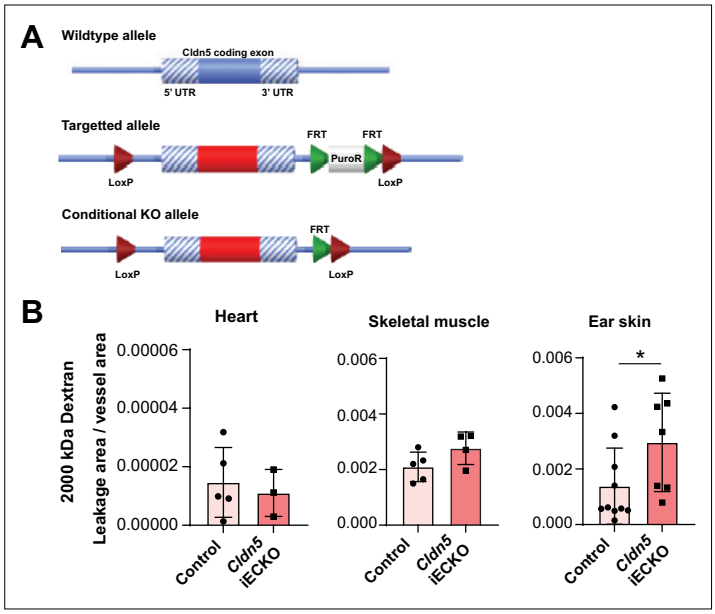

Figure 3—figure supplement 1. (**A**) Schematic diagram showing the targeting strategy of *Cldn5* floxed mice. (**B**) Quantification of histamine-induced (10 mg/kg) leakage of 2000 kDa dextran from the heart, skeletal muscle and ear skin vasculature in control and *Cldn5* iECKO mice. n≥3 mice, 3 or more fields of view/mouse. Error bars; mean ± SD. Statistical significance: two-tailed paired Student's t test.

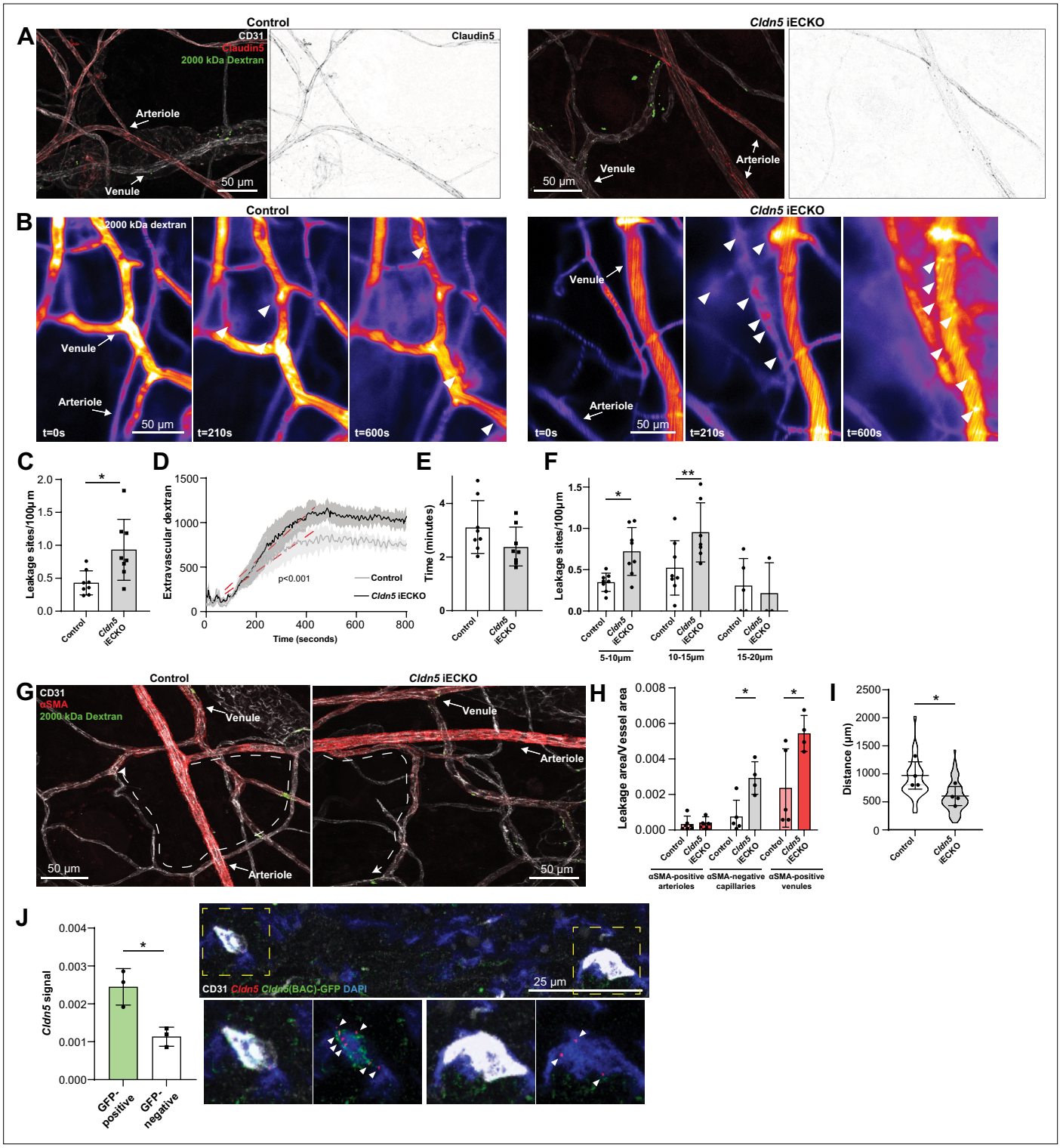

Figure 4. Loss of Claudin5 differentially affects vessel subtypes in the ear dermis. (**A**) Representative images of histamine-induced 2000 kDa dextran leakage in the ear skin of control (left) and *Cldn5* iECKO (right) mice. (**B**) Representative time-lapse images of 2000 kDa dextran leakage in response to intradermal histamine stimulation in the ear skin of control (left) and *Cldn5* iECKO (right) mice. Arrowheads show sites of leakage. (**C**) Leakage sites per vessel length in response to intradermal histamine stimulation in the ear skin of control and *Cldn5* iECKO mice. n≥7 mice, two or more acquisitions/mouse. (**D**) Quantification of extravascular 2000 kDa dextran over time in the ear skin of control and *Cldn5* iECKO mice following intradermal histamine stimulation. Red dashed lines represent lines of best fit for the slope between leakage initiation and leakage termination. n≥7 mice, two or more acquisitions/mouse. (**E**) Lag period between intradermal histamine injection and initiation of leakage in the ear skin of control and *Cldn5* iECKO mice.

Figure 4 continued on next page

Figure 4 continued

n≥7 mice, two or more acquisitions/mouse. (**F**) Leakage sites per length of post-arteriolar vessels of different diameter in response to intradermal histamine stimulation in the ear skin of control and *Cldn5* iECKO mice. n≥7 mice, two or more acquisitions/mouse. n≥7 mice, two or more acquisitions/mouse. (**G**) Representative images of 2000 kDa dextran leakage in response to systemic histamine stimulation in the ear skin of control and *Cldn5* iECKO mice counter-stained for αSMA. Dashed lines with arrows show distance from arteriolar/capillary transition to first site of leakage. (**H**) Leakage area/vessel area of 2000 kDa dextran in response to systemic histamine stimulation in αSMA-positive arterioles, αSMA-negative capillaries and αSMA-positive venules in the ear skin of control and *Cldn5* iECKO mice. n≥4 mice, 3 or more fields of view/mouse. (**I**) Distance between arteriolar-capillary branch points and the first site of 2000 kDa dextran leakage in response to systemic histamine stimulation in the ear skin of control and *Cldn5* iECKO mice. n≥4 mice, 3 or more fields of view/mouse. (**J**) *Cldn5* mRNA expression in *Cldn5*(BAC)-GFP-positive and -negative vessels of the ear skin. Left, quantification of *Cldn5* signal (*Cldn5* mRNA particles/vessel area). Right, representative image. Dashed boxes are magnified below, arrowheads mark *Cldn5* mRNA particles. n=3 mice, 4 or more fields of view/mouse. Error bars; mean ± SD. Statistical significance: two-tailed paired Student's t test (**C, E–J**) and linear regression and ANCOVA (**D**).

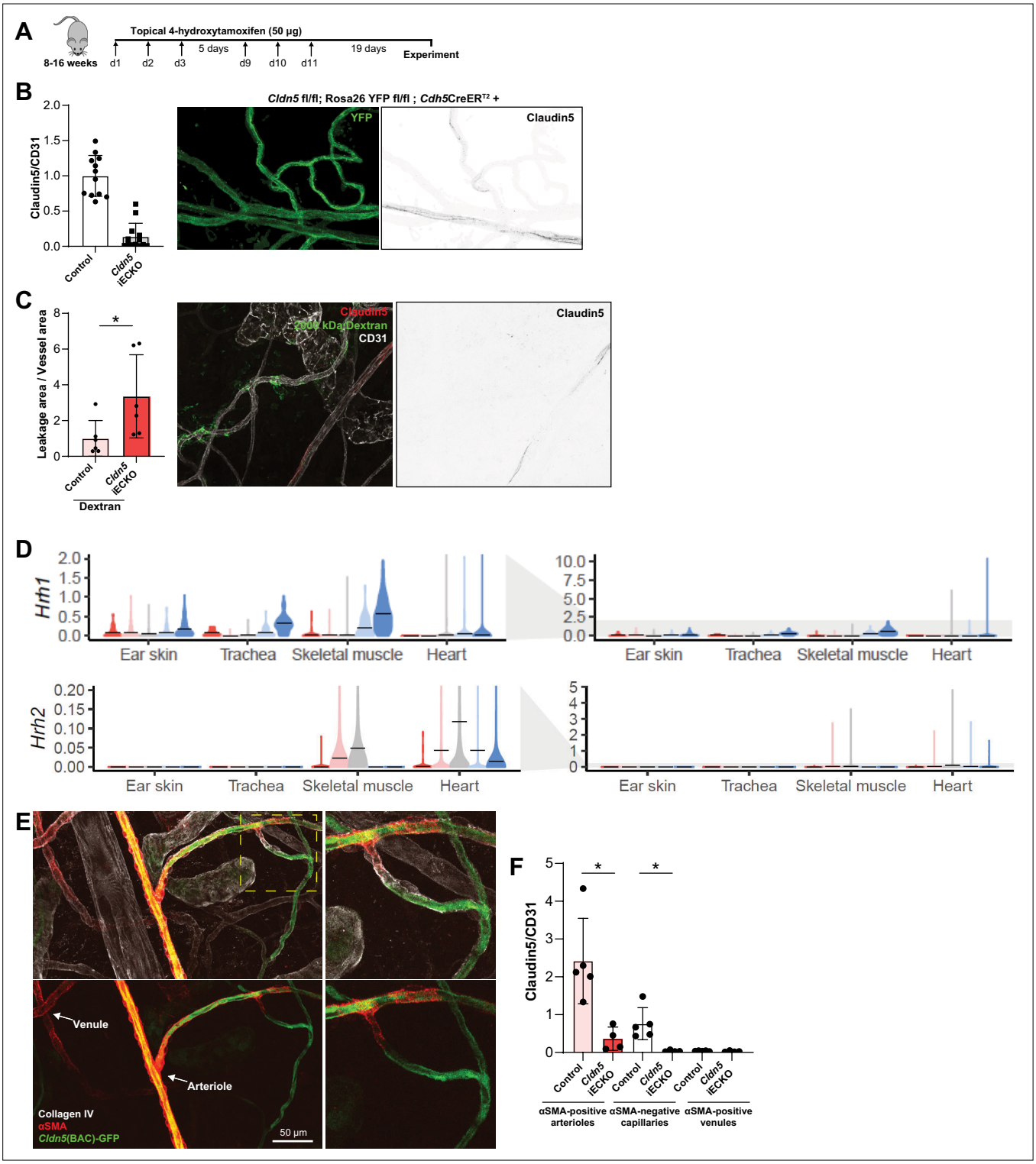

Figure 4—figure supplement 1. (**A**) Schematic illustration of topical 4-hydroxytamoxifen regime. (**B**) Claudin5 protein expression in the ear skin of control and *Cldn5* iECKO mice following topical tamoxifen treatment. Left, quantification. Right, representative image of Claudin5 expression in *Cldn5* $^{fl/fl}$; *Rosa26*$^{lox\text{-}STOP\text{-}lox\text{-}YFP}$; *Cdh5*^{CreERT2} mice following tamoxifen treatment. (**C**) Leakage of 2000 kDa dextran in the ear skin of topically tamoxifen treated control or *Cldn5* iECKO mice in response to histamine (10 mg/kg). Left, quantification. Right, representative image of leakage and Claudin5. (**D**) Violin plots for gene expression of histamine receptors *Hrh1* and *Hrh2*. Gene expression was normalized to account for differences in sample library size and imputed to account for dropouts in the data as described in Methods. (**E**) Image showing the expression of *Cldn5*(BAC)-GFP and αSMA in the mouse ear dermis. Dashed box is shown magnified to right. (**F**) Quantification of Claudin5 expression in αSMA-positive arterioles, αSMA-negative capillaries and αSMA-positive venules in control and *Cldn5* iECKO mice. Error bars; mean ± SD. Statistical significance: two-tailed paired Student's t test.

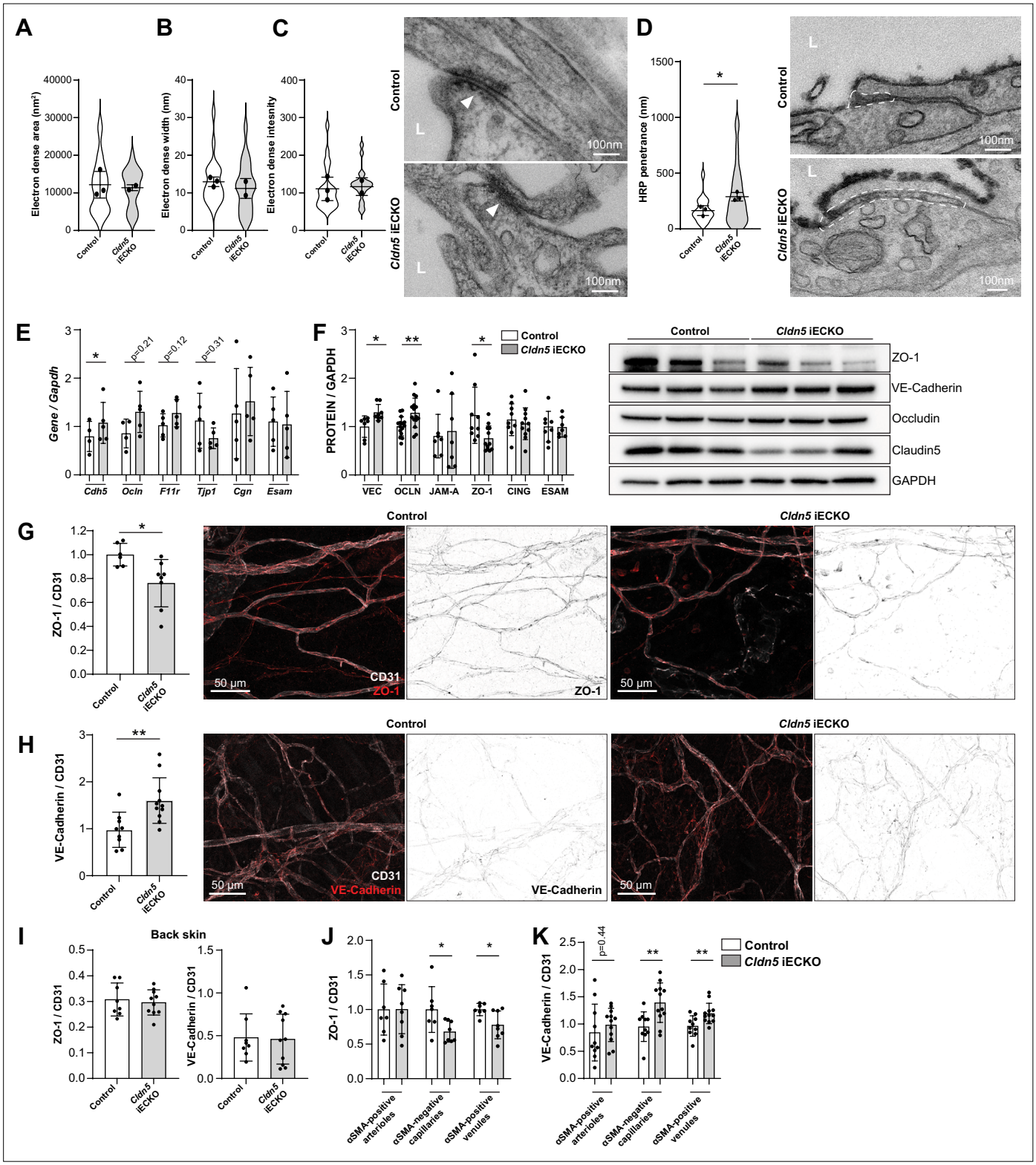

Figure 5. Claudin5 regulates junction protein expression. (**A–C**) Area (**A**) width (**B**) and intensity (**C**) of electron dense regions in the ear skin of control and *Cldn5* iECKO mice after visualisation by TEM. Right, representative TEM images of junctions in the ear skin of control and *Cldn5* iECKO mice. Junctions can be seen within electron dense regions (arrowheads). L, lumen. n≥2 mice, 6 or more fields of view/mouse. (**D**) Distance of HRP penetrance into EC junctions in the ear skin of control and *Cldn5* iECKO mice following systemic histamine stimulation. Right, representative TEM images of HRP penetrance (visualised by electron dense 3,3′-Diaminobenzidine (DAB) reaction precipitate) into EC junctions in the ear skin of control and *Cldn5* iECKO

Figure 5 continued on next page

Figure 5 continued

mice following systemic histamine stimulation. Dashed regions show areas of disrupted junction into which HRP has penetrated. Note that the typical electron dense area is lacking due to absence of uranyl acetate staining. L, lumen. n≥2 mice, 6 or more fields of view/mouse. (**E**) Gene expression of AJ- and TJ-associated genes in lung lysates of control and *Cldn5* iECKO mice. n≥4 mice. (**F**) Expression of AJ- and TJ- associated proteins in lung lysates of control and *Cldn5* iECKO mice. Right, representative western blots of AJ- and TJ- associated proteins in lung lysates of control and *Cldn5* iECKO mice. n≥4 mice. (**G**) Expression of ZO-1 in ear skin blood vessels of control and *Cldn5* iECKO mice. Left, quantification of ZO-1. Right, representative images of ZO-1 in the ear skin of control and *Cldn5* iECKO mice. n≥6 mice, 3 or more fields of view/mouse. (**H**) Expression of VE-Cadherin in ear skin blood vessels of control and *Cldn5* iECKO mice. Left, quantification of VE-Cadherin. Right, representative images of VE-Cadherin in the ear skin of control and *Cldn5* iECKO mice. n≥9 mice, 3 or more fields of view/mouse. (**I**) Quantification of ZO-1 (left) and VE-Cadherin (right) in back skin blood vessels of control and *Cldn5* iECKO mice. n≥8 mice, 2 or more fields of view/mouse. (**J**) Quantification of ZO-1 in different vessel subtypes in the ear skin of control and *Cldn5* iECKO mice. n≥3 mice, 3 or more fields of view/mouse. (**K**) Quantification of VE-Cadherin in different vessel subtypes in the ear skin of control and *Cldn5* iECKO mice. n≥3 mice, 3 or more fields of view/mouse. Error bars; mean ± SD. Statistical significance: two-tailed paired Student's t test.

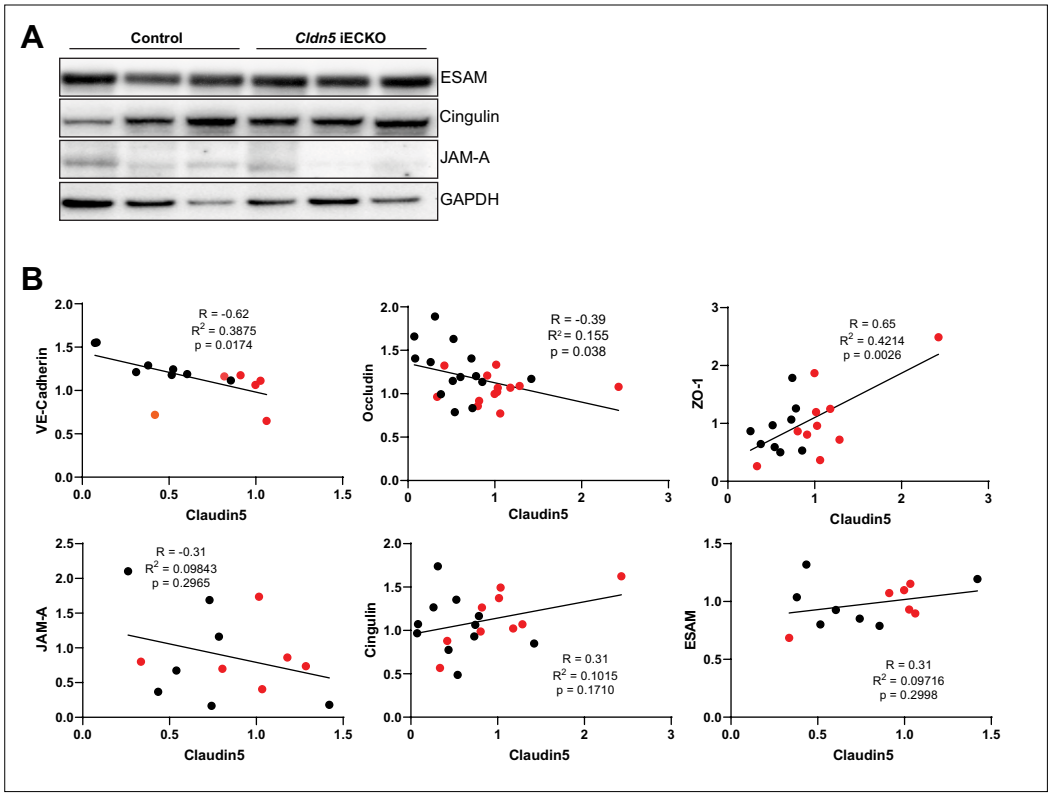

Figure 5—figure supplement 1. (**A**) Representative western blots of ESAM, Cingulin and JAM-A expression in control and *Cldn5* iECKO mouse lung lysates. (**B**) Scatter graphs showing the correlation between Claudin5 expression levels and other EC junction proteins in mouse lung lysates. Both control (red dots) and *Cldn5* iECKO (black dots) mice are represented. Line of best fit following linear regression analysis is shown.